Acta Crystallographica Section F
Structural Biology and Crystallization Communications
ISSN 1744-3091

Crystallization and preliminary X-ray crystallographic analysis of the human kindlin-2 PH domain

Jun Hyuck Lee,[a]*‡ Jun Yop An,[b]‡ HaJeung Park,[c] Hak Jun Kim[a,d] and Soo Hyun Eom[b]

[a]Korea Polar Research Institute, Incheon 406-840, Republic of Korea, [b]School of Life Sciences, Gwangju Institute of Science and Technology, Gwangju 500-712, Republic of Korea, [c]Department of Cancer Biology, The Scripps Research Institute, Jupiter, FL 33458, USA, and [d]Department of Polar Science, University of Science and Technology, Incheon, 406-840, Republic of Korea

‡ These authors contributed equally to this work.

Correspondence e-mail: junhyucklee@kopri.re.kr

Received 7 February 2011
Accepted 12 April 2011

Kindlins contribute to the correct assembly of integrin-containing focal adhesion sites through their direct interaction with the cytoplasmic tail of β-integrin. The FERM domain of kindlins has a unique subdomain organization: the F2 subdomain harbours a centrally located pleckstrin homology (PH) domain that is thought to be involved in the membrane targeting of kindlins. FERM domains are found in a number of cytoskeletal proteins that mediate the interaction between integrins and cytosolic proteins. In the present study, the PH domain of human kindlin-2 was subcloned, solubly expressed in *Escherichia coli* and crystallized using the hanging-drop vapour-diffusion method. A diffraction data set was collected at 2.8 Å resolution using synchrotron radiation on BL-4A at the Pohang Accelerator Laboratory (Pohang, Republic of Korea).

1. Introduction

The kindlin family (kindlin-1, kindlin-2 and kindlin-3) of cytoplasmic proteins localize within integrin-containing cell-adhesion complexes, where they regulate integrin-mediated signalling *via* direct interaction with the C-terminal tail region of β-integrin (Meves *et al.*, 2009). Integrins are heterodimeric adhesion receptors consisting of α and β subunits whose function is to connect cells to substrates in their extracellular environment. The ectodomains of integrins interact with extracellular matrix (ECM) proteins such as fibronectin and laminin, while their short cytoplasmic tails mediate connections to the actin cytoskeleton *via* adaptor proteins such as talin and kindlin (Meves *et al.*, 2009; Moser *et al.*, 2009; Malinin *et al.*, 2010). Interestingly, the site at which kindlin binds to integrin is different from and independent of the talin-binding site. Whereas the F3 domain of talin directly interacts with the membrane-proximal NP*X*Y motif (739-WDTAN-NPLYDEA-750 region) of the β3-integrin cytoplasmic tail, kindlin binds to the membrane-distal N*XX*Y motif (751-TSTFTNITY-759) of the β3-integrin cytoplasmic tail (Larjava *et al.*, 2008; Ma *et al.*, 2008).

Kindlin-family members all possess an atypical FERM (band 4.1/ezrin/radixin/moesin) domain which is split within the F2 subdomain by the insertion of a pleckstrin homology (PH) domain. This is likely to add PH-domain function to the FERM domain of kindlins. Despite minimal sequence homology, the three-dimensional structures of PH domains are remarkably conserved and all possess seven β-strands and a C-terminal α-helix (Rebecchi & Scarlata, 1998; Goult *et al.*, 2009). Most PH domains interact with various phospholipids and are therefore involved in the targeting of proteins to the membrane. The kindlin PH domain is thought to act similarly.

The expression patterns of the three kindlin isoforms are not identical. Whereas kindlin-1 is highly expressed in skin and intestine, kindlin-2 is expressed ubiquitously throughout the body (Ashton *et al.*, 2004). Kindlin-3 is expressed exclusively in haematopoietic cells and its mutation has been linked to leukocyte adhesion deficiency syndrome (Krüger *et al.*, 2008; Moser *et al.*, 2008).

Previous studies have suggested that kindlin-2 mediates an important connection between cell–ECM adhesion sites and the actin cytoskeleton. Moreover, the loss of kindlin-2 in mice results in peri-

Table 1
Data-collection statistics.

Values in parentheses are for the last resolution shell.

X-ray source	PAL-4A
Space group	*C*222
Unit-cell parameters (Å)	a = 50.1, b = 136.8, c = 40.2
Wavelength (Å)	1.0000
Resolution range (Å)	50–2.8 (2.85–2.80)
No. of observed reflections	19002
No. of unique reflections	3540
Completeness (%)	97.7 (92.0)
Multiplicity	5.4 (5.9)
$R_{\rm merge}$†	0.071 (0.312)
$\langle I/\sigma(I)\rangle$	39.3 (8.2)

† $R_{\rm merge} = \sum_{hkl}\sum_i |I_i(hkl) - \langle I(hkl)\rangle| / \sum_{hkl}\sum_i I_i(hkl)$, where $I(hkl)$ is the intensity of reflection hkl, $\sum_{hkl}$ is the sum over all reflections and $\sum_i$ is the sum over i measurements of reflection hkl.

implantation lethality caused by impaired integrin activation, which in turn leads to delayed cell spreading (Montanez *et al.*, 2008). To further investigate the functional roles of the kindlin-2 PH domain, we are carrying out a structure–function analysis of human kindlin-2. As a first step towards its structural characterization, we report the preliminary results of a crystallographic examination of the kindlin-2 PH domain.

2. Materials and methods

2.1. Cloning, expression and purification of the kindlin-2 PH domain

The nucleotide sequence encoding the human kindlin-2 PH domain (amino acids 383–503) was amplified and subcloned into the *Nde*I/*Xho*I sites of the pET-28a vector, which contains an N-terminal hexahistidine tag and thrombin cleavage site. The cells were induced with 1 m*M* IPTG, incubated overnight and collected by centrifugation at 3540*g* for 15 min. The cell pellet was suspended in lysis buffer (50 m*M* sodium phosphate pH 8.0, 300 m*M* NaCl and 5 m*M* imidazole) and lysed by sonication. The resultant lysate was pelleted by centrifugation at 13 600*g* for 20 min, after which the supernatant was loaded onto a gravity-flow column (Bio-Rad) packed with Ni–NTA affinity resin (Peptron) pre-equilibrated with lysis buffer. The column and matrix were then washed with ten column volumes of lysis buffer and the N-terminal His-tag fusion protein was eluted using a solution consisting of 50 m*M* sodium phosphate pH 8.0, 300 m*M* NaCl and 300 m*M* imidazole. After cleavage of the hexahistidine tag at 277 K overnight, the proteins were applied onto a Superdex-75 column (Amersham Biosciences) equilibrated with a solution consisting of 20 m*M* Tris–HCl pH 8.0 and 150 m*M* NaCl. Fractions containing the kindlin-2 PH domain were collected and concentrated by ultrafiltration to 21.8 mg ml^{-1} using Centricon-10 (Amicon). The protein concentration was determined spectrophotometrically using an extinction coefficient of 23 950 M^{-1} cm^{-1} (MW = 13 849 Da) at 280 nm. The final purified product included an additional sequence GSHM at its N-terminus owing to a cloning artifact.

2.2. Crystallization and data collection

The kindlin-2 PH domain was crystallized at 293 K using the hanging-drop vapour-diffusion method. The crystals were grown on a siliconized cover slip by equilibrating a mixture containing 1 µl protein solution (21.8 mg ml^{-1} protein in 20 m*M* Tris–HCl pH 8.0 and 150 m*M* NaCl) and 1 µl reservoir solution [0.1 *M* Tris–HCl pH 8.5, 30%(*w*/*v*) PEG 4000, 0.2 *M* lithium sulfate] against 0.5 ml reservoir solution. A single crystal formed after 3 d and grew to a largest dimension of 0.3 mm.

For cryogenic experiments, a suitable cryoprotectant was determined to be reservoir solution plus 10%(*w*/*v*) glycerol. The crystals were flash-cooled by plunging the loop into liquid nitrogen and were allowed to equilibrate for 1 min. A native data set was collected to 2.8 Å resolution on beamline BL-4A at the Pohang Accelerator Laboratory (Pohang, Republic of Korea) using an X-ray beam at a single wavelength (1.0000 Å). The crystal was exposed for 3 s per 1.0° rotation in ω at a crystal-to-detector distance of 280 mm. Diffraction images were recorded on an ADSC Quantum 315 CCD detector,

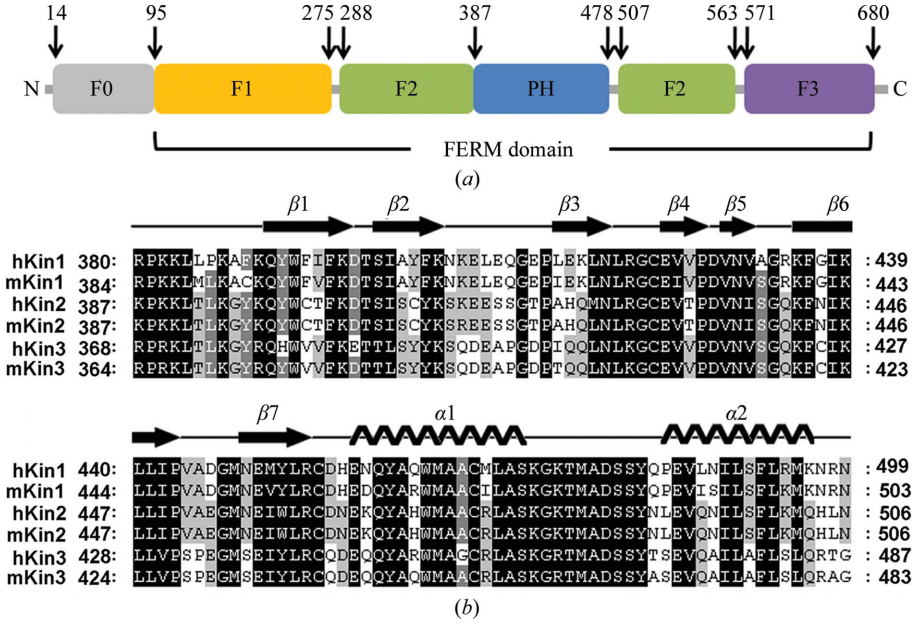

Figure 1
Domain structure of human kindlin-2. (*a*) Cartoon representation showing the domain arrangement of human kindlin-2. The kindlin-2 PH domain is indicated by a blue box. (*b*) Multiple sequence alignment of the PH domains of human and mouse kindlins using *ClustalX* (Thompson *et al.*, 1997). Highly conserved residues are shaded grey and black. The secondary-structural elements within the kindlin-2 PH-domain sequence predicted using the *Phyre* server (Kelley & Sternberg, 2009) are shown above the alignments.

scanning a total of 208° rotation in ω. The data set was indexed and processed using *HKL*-2000 (Otwinowski & Minor, 1997). Data-collection statistics are given in Table 1.

3. Results

Multiple sequence alignment of human and mouse kindlin proteins revealed that the PH domain is well conserved across all three kindlin isoforms (Fig. 1). Typical PH-domain structures include seven antiparallel β-strands capped at the C-terminus by an amphiphilic α-helix. Notably, however, the secondary structures predicted from amino-acid sequence alignment of kindlin PH domains indicated that our crystallized kindlin-2 PH domain has an additional C-terminal helix (α2) which is highly conserved in all three kindlin-family proteins. It is also noteworthy that about ten amino acids between the α1 and α2 helices (amino-acid residues 476–485) are highly conserved, indicating the importance of this loop region (Fig. 1*b*).

The recombinant kindlin-2 PH domain was expressed in *E. coli* BL21 (DE3) as a soluble fraction and purified with a yield of about 30 mg protein per litre of culture (Fig. 2*a*). Native crystals with approximate dimensions of 0.05 × 0.05 × 0.15 mm were obtained within 7 d using the reservoir solution mentioned above (Fig. 2*b*). The kindlin-2 PH-domain crystal belonged to space group *C*222 (unit-cell parameters a = 50.1, b = 136.8, c = 40.2 Å) and diffracted to 2.8 Å resolution (Fig. 2*c*). Assuming one molecule per asymmetric unit, the Matthews coefficient (V_M) was calculated to be 2.49 Å^3 Da^{-1}, which corresponds to a solvent content of 50.6% (Matthews, 1968).

We initially attempted to use molecular-replacement methods for phase determination with the *MOLREP* (Vagin & Teplyakov, 2010) and *Phaser* (McCoy *et al.*, 2007) programs. However, this approach failed to provide correct solutions for either the molecular orientation or the molecular packing, despite the availability of NMR structures of the kindlin-3 PH domain (Moser *et al.*, 2008; amino-acid residues 349–482; PDB entry 2ys3; 67% sequence identity) and the Kiaa1914 PH domain (Xu *et al.*, 2007; PDB entry 2cof; 24% sequence identity) as search models. Initially, we tried to solve the structure by molecular replacement using the coordinates of either ensembles of 20 NMR models or a single NMR model. For cross-rotation function calculation we used data in the resolution range 15–3.5 Å. Unfortunately, the cross-rotation search with these NMR models did not yield a solution. Next, we produced polyalanine and loop-truncated models derived from the NMR structures and performed more than 30 MR calculations with varying parameters. Unfortunately, we could not obtain a solution with the NMR models even though the search model had 60% sequence identity to the kindlin-2 PH domain. This

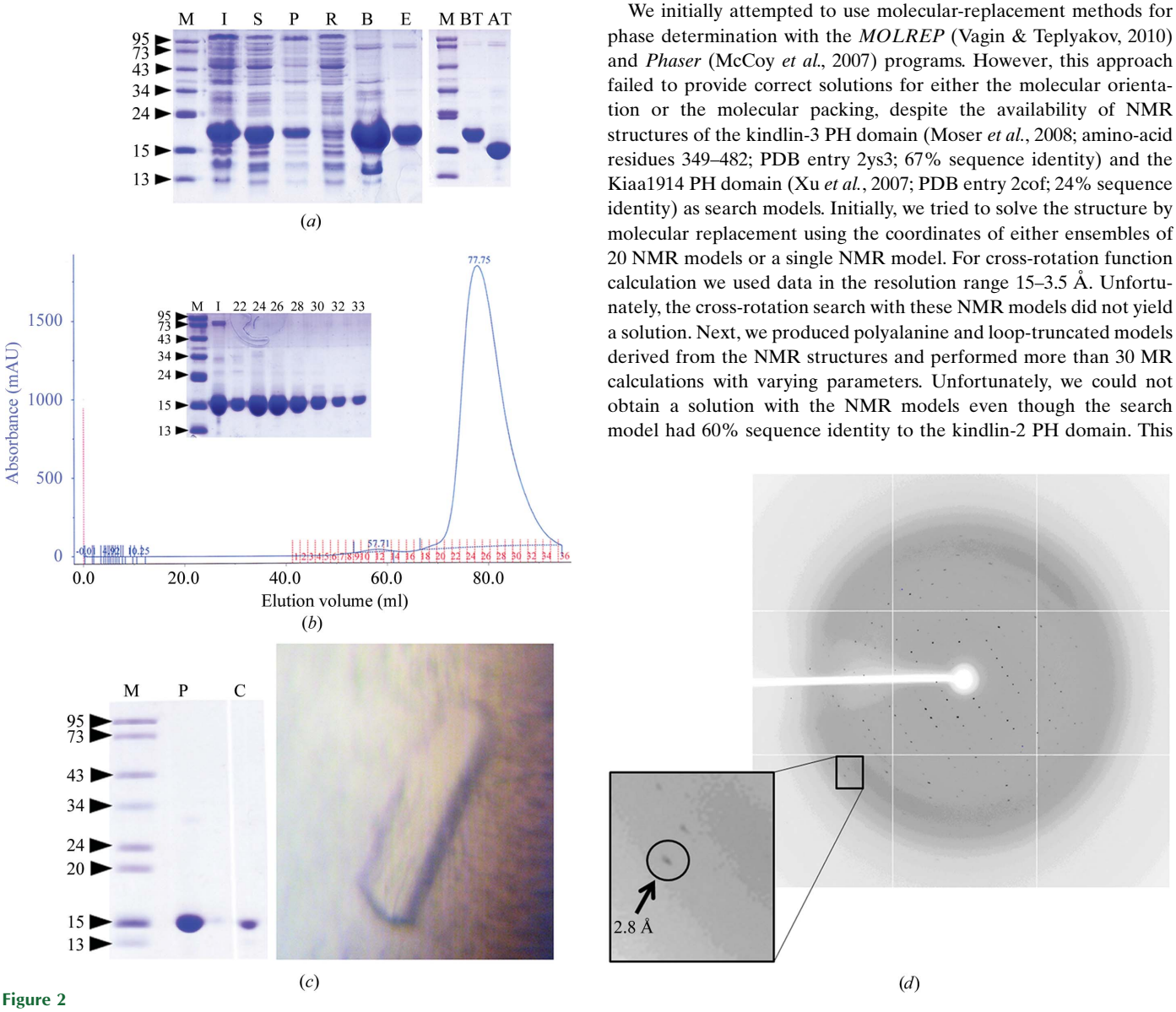

Figure 2
(*a*) 15% SDS–PAGE analysis of recombinant kindlin-2 PH domain expression and purification. Lane M, protein molecular-weight markers (kDa); lane I, total protein after IPTG induction; lane S, supernatant fraction after IPTG induction; lane P, pellet fraction after IPTG induction; lane R, flowthrough during hexahistidine-tag affinity chromatography; lane B, hexahistidine-tag bead after washing; lane E, elution with 200 m*M* imidazole; lane BT, before thrombin digestion; lane AT, after thrombin digestion at 277 K overnight. (*b*) Size-exclusion chromatography profile of the kindlin-2 PH domain on a Superdex 75 column. The injected sample and several fractions are visualized on a 15% SDS–PAGE gel (inset). The elution volume indicated that the kindlin-2 PH domain behaves as a monomer in solution with an apparent molecular weight of 21 kDa. (*c*) A crystal of the kindlin-2 PH domain (right) grown for 3 d in 0.1 *M* Tris–HCl pH 8.5, 30%(*w*/*v*) PEG 4000, 0.2 *M* lithium sulfate. Its approximate dimensions are 0.05 × 0.05 × 0.15 mm. The results of the 15% SDS–PAGE analysis (left) showed that the dissolved crystals (lane C) contain a protein with the same molecular weight as the purified kindlin-2 PH domain (lane P), indicating that no degradation occurred during the crystallization. (*d*) X-ray diffraction pattern (2.8 Å resolution) of a crystal of the kindlin-2 PH domain.

could be a consequence of structural differences between the solution structure and the crystalline state. As the kindlin-2 PH domain contains five methionine residues, attempts to solve the structure using the MAD (multiwavelength anomalous dispersion) method with selenomethionine-labelled protein are now in progress.

We thank the beamline staff at BL-4A of Pohang Accelerator Laboratory (Pohang, Republic of Korea) for their kind help with data collection. The work was supported by Korea Polar Research Institute Grant No. PG10010 (to HJK), the Korea Healthcare Technology R&D Project, Ministry for Health, Welfare and Family Affairs (A092006 to SHE) and a GIST Systems Biology Infrastructure Establishment Grant (2011 to SHE).

References

Ashton, G. H. *et al.* (2004). *J. Invest. Dermatol.* **122**, 78–83.
Goult, B. T., Bouaouina, M., Harburger, D. S., Bate, N., Patel, B., Anthis, N. J., Campbell, I. D., Calderwood, D. A., Barsukov, I. L., Roberts, G. C. & Critchley, D. R. (2009). *J. Mol. Biol.* **394**, 944–956.
Kelley, L. A. & Sternberg, M. J. (2009). *Nature Protoc.* **4**, 363–371.
Krüger, M., Moser, M., Ussar, S., Thievessen, I., Luber, C. A., Forner, F., Schmidt, S., Zanivan, S., Fässler, R. & Mann, M. (2008). *Cell*, **134**, 353–364.
Larjava, H., Plow, E. F. & Wu, C. (2008). *EMBO Rep.* **9**, 1203–1208.
Ma, Y.-Q., Qin, J., Wu, C. & Plow, E. F. (2008). *J. Cell Biol.* **181**, 439–446.
Malinin, N. L., Plow, E. F. & Byzova, T. V. (2010). *Blood*, **115**, 4011–4017.
Matthews, B. W. (1968). *J. Mol. Biol.* **33**, 491–497.
McCoy, A. J., Grosse-Kunstleve, R. W., Adams, P. D., Winn, M. D., Storoni, L. C. & Read, R. J. (2007). *J. Appl. Cryst.* **40**, 658–674.
Meves, A., Stremmel, C., Gottschalk, K. & Fässler, R. (2009). *Trends Cell Biol.* **19**, 504–513.
Montanez, E., Ussar, S., Schifferer, M., Bösl, M., Zent, R., Moser, M. & Fässler, R. (2008). *Genes Dev.* **22**, 1325–1330.
Moser, M., Legate, K. R., Zent, R. & Fässler, R. (2009). *Science*, **324**, 895–899.
Moser, M., Nieswandt, B., Ussar, S., Pozgajova, M. & Fässler, R. (2008). *Nature Med.* **14**, 325–330.
Otwinowski, Z. & Minor, W. (1997). *Methods Enzymol.* **276**, 307–326.
Rebecchi, M. J. & Scarlata, S. (1998). *Annu. Rev. Biophys. Biomol. Struct.* **27**, 503–528.
Thompson, J. D., Gibson, T. J., Plewniak, F., Jeanmougin, F. & Higgins, D. G. (1997). *Nucleic Acids Res.* **25**, 4876–4882.
Vagin, A. & Teplyakov, A. (2010). *Acta Cryst.* D**66**, 22–25.
Xu, J., Bai, X.-H., Lodyga, M., Han, B., Xiao, H., Keshavjee, S., Hu, J., Zhang, H., Yang, B. B. & Liu, M. (2007). *J. Biol. Chem.* **282**, 16401–16412.